Theory of dynamical cavitation threshold for diesel fuel atomization

Fujikawa, Toshihide; Egashira, R.; Hooman, K.; Yaguchi, H.; Masubuchi, H.; Fujikawa, S.

DOI
10.1088/1873-7005/ac830d

Publication date
2022

Document Version
Final published version

Published in
Fluid Dynamics Research

PAPER

Theory of dynamical cavitation threshold for diesel fuel atomization

IOP Publishing | The Japan Society of Fluid Mechanics Fluid Dynamics Research

Fluid Dyn. Res. **54** (2022) 045505 (16pp) https://doi.org/10.1088/1873-7005/ac830d

Theory of dynamical cavitation threshold for diesel fuel atomization

Toshihide Fujikawa[1,*], R Egashira[2], K Hooman[3], H Yaguchi[4], H Masubuchi[5] and S Fujikawa[6]

[1] Department of Mechanical Engineering, Miyakonojo College, National Institute of Technology (KOSEN), 473-1 Yoshio-cho, Miyakonojo, Miyazaki, 885-8567, Japan,
[2] Department of Intelligent Mechanical Engineering, Fukuoka Institute of Technology, 3-30-1 Wajiro-higashi, Higashi-ku, Fukuoka 811-0295, Japan
[3] Department of Process and Energy, Delft University of Technology, Delft, 2628 CB, The Netherlands
[4] Department of Mechanical Engineering, Gunma College, National Institute of Technology (KOSEN), 580 Toriba-machi, Maebashi, Gunma 371-8530, Japan
[5] Department of Mechanical Engineering, Oyama College, National Institute of Technology (KOSEN), 771 Nakakuki, Oyama, Tochigi 323-0806, Japan
[6] Hokkaido University, Kita 8, Nishi 5, Kita-ku, Sapporo, Hokkaido 060-0808, Japan

E-mail: fujikawa@cc.miyakonojo-nct.ac.jp

Received 8 May 2022; revised 23 June 2022
Accepted for publication 21 July 2022
Published 1 August 2022

Communicated by Professor Hyung Jin Sung

Abstract

Theory of dynamical cavitation threshold for vapor and non-condensable gas bubble nuclei is proposed based on a model equation constructed from Rayleigh–Plesset equation for glycerol, the liquid with viscosity higher than that of water by 1500 times, under a finite duration of strong tension. The model equation is ascertained to be valid in cases of strong tension under which cavitation occurs. Our model enables the study of dynamics of nuclei on the phase plane of the nucleus radius and the growth velocity, by which the full details of the threshold are revealed. We propose a dimensionless parameter to be used to classify the threshold of cavitation. Our model offers a simple mathematical expression to calculate the maximum radii attained, while under tension, for each of these three recognized patterns. For each observed pattern, we present unique predictive correlations for the radius of the nucleus growing for the tension duration. Moreover, we elucidate that the dynamics of the nuclei, grown up to certain sizes, is fully controlled by tension independent of the viscosity. The discrepancy between the dynamical threshold and the

* Author to whom any correspondence should be addressed.

conventional Blake's threshold is discussed. Finally, the utility of the theory presented here is demonstrated through numerical examples.

Keywords: diesel fuel atomization, dynamical cavitation threshold, bubble dynamics

1. Introduction

Cavitation is the formation and subsequent growth of bubble nuclei contained in liquids when liquid pressure drops below the saturated vapor pressure (Young 1999, Franc and Michel 2005, Brennen 2013). The pressure reduction can be caused by high-speed flows of liquids or tension imposed on them. For example, 1 MPa tension can be induced for a hundred microseconds downstream of a cylinder installed within a duct when the liquid passing through the narrow slit between the cylinder surface and duct walls flew at about 50 m s^{-1} (Washio 2014). Such flow provides us a situation suitable for fundamental study on cavitation threshold based on bubble dynamics—formation, growth, and translation of bubble nuclei. However, whether cavitation takes place due to the fracture of water without pre-existence of the nuclei, as Washio insists, is possible or not still remains vague. The theoretical tension strength of water at room temperature is about 100 MPa, suggesting that acoustically induced cavitation would require a sound pressure of at least 100 MPa (Young 1999). On the other hand, cavitation is observed with pressure amplitudes of about 0.1 MPa in water, implying the presence of pre-existing nuclei (Mørch 2015, Yasui 2018). Despite the uncertainty about the effects and pre-existence of the nuclei, the method Washio proposed is quite suitable for the study of the threshold if it is assisted with a threshold theory based on bubble dynamics.

Cavitation can also occur in internal flows, for instance, within fuel injector nozzles of diesel engines. It plays an important role in promoting the breakup of fuel jets, where the fuel is pressurized to and above 100 MPa to be suddenly depressurized. This will thereby result in strong tension (around 10 MPa) and; consequently, cavitation (Sun *et al* 2021). Cavitation can effectively control and promote fuel atomization. It is an impending issue for design and optimization of the injector nozzles. Gianndakis *et al* (2008) presented informative results on cavitation threshold in the nozzles by computational fluid dynamics (CFD) coupled with bubble dynamics taking account of translational motion of bubble nuclei. However, why initial radii of the nuclei assumed to pre-exist, as they pointed out by CFD simulation, do not affect the threshold at all is to be understood. A crucial issue common to Gianndakis *et al'* method and Washio's one mentioned above is the lack of understanding of the physics of threshold in theoretical and numerical investigations. Despite this, studies of these nature on the cavitation threshold might be remarkably advanced if a new perspective theory of the threshold under tension is constructed based on bubble dynamics in an analytical manner and incorporated into Gianndakis *et al'* method or that of Washio.

Considering the above-mentioned situations of cavitation threshold, we understand that construction of a new theory of cavitation threshold is impending. There is currently no theory on the dynamics of the threshold although the threshold has been discussed on the growth of a bubble nucleus in a quasistatic process as Blake's threshold (Young 1999, Franc and Michel 2005, Brennen 2013). Blake's threshold is not a dynamical one—temporal factor on the nucleus growth and viscosity effect of the liquid are not taken into account. On the contrary, cavitation actually occurs in viscous liquids under tension or positive pressures lower than saturated vapor pressures during finite times. For example, again in case of Gianndakis *et al'* study (2008), cavitation is caused by very short (only for microseconds) transient strong

tension (of about 10 MPa in magnitude). Blake's threshold is of no use for such cavitation problems. This is the reason why the authors stick to construct a new theory on the threshold, i.e. 'dynamical cavitation threshold,' taking account of both temporal factor of the growth and viscosity of the liquid in an analytical manner based on bubble dynamics.

This paper focusses solely on bubble dynamics study to provide insight into the dynamical cavitation threshold of vapor and non-condensable gas bubbles—bubble nuclei—in glycerol under a finite duration of strong tension for diesel fuel atomization. No serious attempt has been made to perform the analysis until the present. It is, indeed, difficult to obtain an exact, analytical solution to the problem. However, with certain reasonable approximations it is possible to obtain the analytical expression for dynamical cavitation threshold for the nuclei. Along this line, the authors will apply the model equation which was constructed based on Rayleigh–Plesset (R-P) equation (Fujikawa *et al* 2019). The trait of our model equation enables us to deal with the dynamics of the nucleus on the phase plane of the nucleus radius and the growth velocity; acceleration term is treated so as not to appear explicitly in the equation. Hence, it is superior to other techniques that aim at directly solving the R-P equation. Our goal is to elucidate what are controlling factors for the threshold of vapor and non-condensable gas bubble nuclei and how large they grow in highly viscous liquids during infinite durations of strong tension. Thereby, we will deduce simple predictive formulae for the threshold. We will clarify the difference between our dynamical threshold and Blake's quasi static one and we will demonstrate how to use our theory. The limitation of the model equation will be discussed and the extension of our model to cases with water as the liquid fluid will be demonstrated.

2. Problem statement, model equation, and its validation and limitation

2.1. Problem statement and model equation

First of all, let us state our problem to be dealt with in the present paper. We suppose that there exists a stationary bubble nucleus in a highly viscous liquid, then the pressure of the liquid surrounding the nucleus is suddenly changed from a high value to a strong tension one. The nucleus begins to grow to a certain size, attaining a visible size—cavitation threshold and we intend to use our model to predict the onset of this threshold.

Figure 1(a) shows the temporal variation of the pressure imposed on the liquid. The abscissa denotes the time t and the ordinate indicates the liquid pressure $p_l(t)$ as a function of time only. At time $t = 0$, the liquid is in the state of a pressure p_{l0} and the nucleus of a radius R_0 is in equilibrium with the liquid, whilst the pressure of the non- condensable gas within the nucleus is p_{g0} and the saturated vapor pressure is p_v. Just at the instant when the liquid is depressurized by $P(>0)$ for a period T in a stepwise fashion, the nucleus begins to grow. During the nucleus growth, the vapor pressure is assumed to remain constant at the ambient liquid temperature. After the period T, the liquid pressure again restores in a stepwise manner to a higher pressure p_a. As shown in figure 1(b), the nucleus grows up to a large bubble with radius R_1 during T and continues to grow for $t \geqslant T$ in the high pressure p_a, attains a maximum radius $R_{\max}$, and then shrinks. In summary, we consider the cavitation threshold in the situation that the stationary nucleus is exposed to strong tension instead of in the situation that the nucleus grows and shrinks in a flowing liquid. Our model is developed for a specific problem where an initial high-pressure state undergoes significant pressure changes leading to strong tension which, in turn, can be linked to injector nozzles. Note in essence that, our theory is not tuned based on the entire liquid pressure history (as the final pressure state is not a model input).

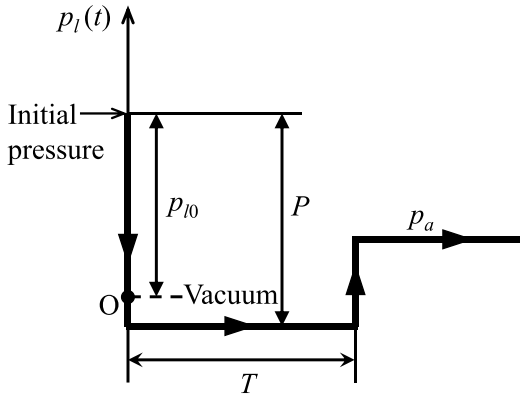

(a) Temporal variation of liquid pressure

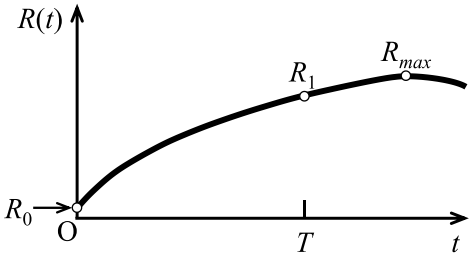

(b) Nucleus radius change

Figure 1. The temporal variation of liquid pressure (a) and the nucleus radius change (b). The liquid is initially in the state of a pressure p_{l0} from which it is depressurized by P during a time T. The liquid subsequently restores to a high pressure p_a. According to the liquid pressure change, the nucleus grows from the radius R_0 to $R_{\max}$via R_1.

We will introduce the following dimensionless quantities with the asterisk:

$$R^* = \frac{R}{R_0},\ t^* = \frac{t}{T},\ p^* = \frac{pT^2}{\rho R_0^2},\ \mu^* = \frac{4\mu T}{\rho R_0^2},\ \sigma^* = \frac{2\sigma T^2}{\rho R_0^3}, \tag{1}$$

where R is the nucleus radius which is a function of time, p is generally expressed to be the pressure (p_a, p_{l0}, P), ρ is the liquid density, μ is the viscosity coefficient of the liquid, and σ is the surface tension coefficient of the liquid. Paying attention to a ratio of μ^* to p^*, we notice that it is in inverse proportion to the tension duration T, for given μ and p. Keeping the viscosity and pressure constant, the tension strength decays as the tension duration is longer, that is, the effect of the viscosity on the nucleus growth becomes less pronounced for the longer tension duration. The liquid is assumed to be incompressible, which is only valid before the threshold. A bubble nucleus is also supposed to exist in the liquid (Young 1999) and we will confine to cavitation threshold under at most 10 MPa according to Gianndakis *et al* (2008).

Then, the R-P equation for the radial motion of the nucleus is given in the dimensionless form as follows (Young 1999, Franc and Michel 2005, Brennen 2013):

$$R\frac{\mathrm{d}^2R}{\mathrm{d}t^2} + \frac{3}{2}\left(\frac{\mathrm{d}R}{\mathrm{d}t}\right)^2 + \frac{\mu}{R}\left(\frac{\mathrm{d}R}{\mathrm{d}t}\right) + \frac{\sigma}{R} - \frac{p_{g0}}{R^3} - p_v + p_l(t) = 0, \tag{2}$$

where the asterisk is dropped and will be omitted hereafter. Initial conditions required to solve (2) are $R(t=0)=1$ and $\mathrm{d}R/\mathrm{d}t(t=0)=0$. The gas is assumed to obey the isothermal law (Fujikawa 1980). As the nucleus is initially in equilibrium with the liquid, the following pressure balance holds: $p_{g0}+p_v=p_{l0}+\sigma$. A sudden drop in the liquid pressure $p_l(t)$ in (2) can be expressed as $p_l(t)=p_{l0}-P$, which means that the liquid is exposed to a tension state for $p_l(t)=p_{l0}-P<0$; tension strength is defined as $\Delta P=P-p_{l0}>0$, i.e. $p_l(t)=-\Delta P$. We should emphasize that cavitation threshold is possible only if $\Delta P\gg 1$. Otherwise, we have $R=\mathrm{O}(1)$. We further need a condition for the initial radius so that the nucleus can start to grow under a given tension strength:

$$\frac{\sigma}{\Delta P+p_{g0}+p_v}<1\,. \tag{3}$$

For convenience, (3) can be expressed as $(R(t=0))_{\mathrm{dim}}>(2\sigma/(\Delta P+p_{g0}+p_v))_{\mathrm{dim}}$ in the dimensional form where the subscript *dim* denotes dimensional quantities, which enables us to understand (3) more intuitively (Fujikawa *et al* 2019).

Making use of an identity $\mathrm{d}^2R/\mathrm{d}t^2=(1/2)\cdot\mathrm{d}(\mathrm{d}R/\mathrm{d}t)^2/\mathrm{d}R$ and $p_l(t)=-\Delta P<0$, (2) can be rewritten as:

$$\frac{1}{2}\frac{\mathrm{d}}{\mathrm{d}R}\left(\frac{\mathrm{d}R}{\mathrm{d}t}\right)^2+\frac{3}{2R}\left(\frac{\mathrm{d}R}{\mathrm{d}t}\right)^2+\frac{\mu}{R^2}\frac{\mathrm{d}R}{\mathrm{d}t}+\frac{\sigma}{R^2}-\frac{p_{g0}}{R^4}-\frac{\Delta P+p_v}{R}=0\,. \tag{4}$$

Equation (4) will be solved subject to two simplifications; i.e. (a) when the acceleration term in (4) is discarded, and, (b) when an inviscid liquid assumption can be made in (4), that is $\mu=0$. In the simplification (a), it compromises accuracy in the nucleus growth, which suggests that validity and limitation of the analysis must be made clear. In view of the assumption (a), we can integrate (4), resulting in:

$$\left(\frac{\mathrm{d}R}{\mathrm{d}t}\right)^2+\frac{2\mu}{3R}\frac{\mathrm{d}R}{\mathrm{d}t}-\frac{2p_{g0}}{3R^3}+\frac{2\sigma}{3R}-\frac{2}{3}(\Delta P+p_v)=0. \tag{5}$$

On the other hand, under the assumption (b), equation (4) can be solved as follows. Since equation (4) for $\mu=0$ is still in an intricate form, it is further transformed into a well-known type of the first-order differential equation by some variable changes, through which the general solution of equation (4) is obtained as:

$$\left(\frac{\mathrm{d}R}{\mathrm{d}t}\right)^2-2p_{g0}\frac{\ln R}{R^3}+\frac{\sigma}{R}+\frac{a}{R^3}-\frac{2}{3}(\Delta P+p_v)=0, \tag{6}$$

where the constant a is an integration constant. Equation (6) is the solution to the R-P equation for the inviscid liquid, thus, correct from the view point of bubble dynamics, whilst (5) solely reveals correct forms on the viscosity term and the inertia terms—the first and last terms. Based on these facts, noticing the forms of (5) and (6) and taking account of the viscous term in (5) into consideration in (6), we obtain:

$$\begin{aligned}&\left(\frac{\mathrm{d}R}{\mathrm{d}t}\right)^2+\frac{2\mu}{3R}\frac{\mathrm{d}R}{\mathrm{d}t}-2p_{g0}\frac{\ln R}{R^3}+\frac{\sigma}{R}\left(1-\frac{1}{R^2}\right)\\&\quad-\frac{2}{3}(\Delta P+p_v)\left(1-\frac{1}{R^3}\right)=0,\end{aligned} \tag{7}$$

where the constant a in (6) is determined from the initial conditions as $a=2(P-p_{l0}+p_v)/3-\sigma$.

We must note that (7) is a model equation based on the simplifications (a) and (b). Comparing (4) with (7), we notice the different points as follows—the viscous term in (7), the factor

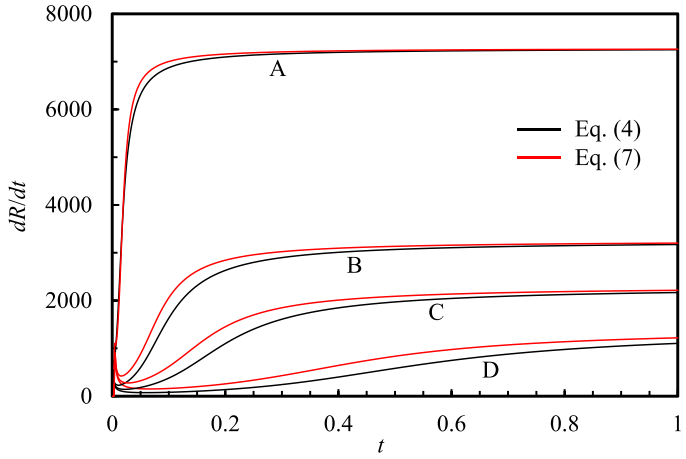

Figure 2. Comparison of equations (4) and (7) for temporal variations of the growth velocity for the nucleus with $R_0 = 1$ ($1\ \mu$m) under different tension strength in glycerol.

$1/R^2$ in the fourth term, and the factor $1/R^3$ in the last term. The two factors are negligibly small when $R \gg 1$ which is the case with cavitation threshold. As for the viscous term in (7), which is crucial, validation and limitation of the model equation must be clarified as will be done by comparing it with (4) in the next subsection.

2.2. Validation and limitation of model equation

To verify the validity and limitation of (7) for highly viscous liquids, we will inspect the growth of a 1 μm-radius nucleus ($R_0 = 1\ \mu$m) in glycerol when glycerol is initially pressurized at 100 MPa and suddenly exposed to tension at 20 °C for 100 μs (Gianndakis *et al* 2008, Sun *et al* 2021). The duration of 100 μs is a time of the nucleus experiencing tension in a 5 mm-tension domain when the flow velocity is 50 m s^{-1}. The tension strength and the duration are set as parameters in this paper. Thermophysical properties (20 °C) are: $\rho = 1.257 \times 10^3$ kg m^{-3}, $\mu = 1.499$ Pa · s, $\sigma = 6.340 \times 10^{-2}$ N m^{-1} and $p_v = 1.160 \times 10^{-2}$ Pa. The following are dimensionless quantities: $p_{l0} = 7.955 \times 10^8$, $\mu = 4.770 \times 10^5$, $\sigma = 1.009 \times 10^6$, $p_v = 9.228 \times 10^{-2}$, and $p_{g0} = p_{l0} - p_v + \sigma = 7.965 \times 10^8$. The constraint given by (3) for the nucleus growth fully holds throughout the paper; the numerical value of the left-hand side of (3) is less than $\sigma/p_{g0} = 1.267 \times 10^{-3}$ for any $\Delta P > 0$. For convenience, the dimensional pressure to 1 in the dimensionless form corresponds to 1.257×10^{-1} Pa (e.g. 100 MPa corresponds to 7.955×10^8) and the dimensional velocity of 1 corresponds to 1×10^{-2} m s^{-1} (e.g. 1 m s^{-1} corresponds to 1×10^2).

Figure 2 compares (4) and (7) on the growth velocity of nucleus up to $t = 1$ (the tension duration) for A: $\Delta P = 7.955 \times 10^7$ (10 MPa in dimensional value), B: $\Delta P = 1.591 \times 10^7$ (2 MPa), C: $\Delta P = 7.955 \times 10^6$ (1 MPa), and D: $\Delta P = 3.022 \times 10^6$ (0.380 MPa). It should be noted that nuclei larger than 1.2 nm in initial radius can grow for the condition of the case A from (3). The last case, case D, may be the lowest limit under which the model equation is (barely) valid for glycerine. The spike-like small protuberance seen near the origin in each case is due to the gas pressure, not due to inaccuracy of calculation (more details on this in section 3.1). The black lines are obtained by solving (4), whilst the red lines are obtained by solving (7). The results demonstrate that the discrepancies between (4) and (7)

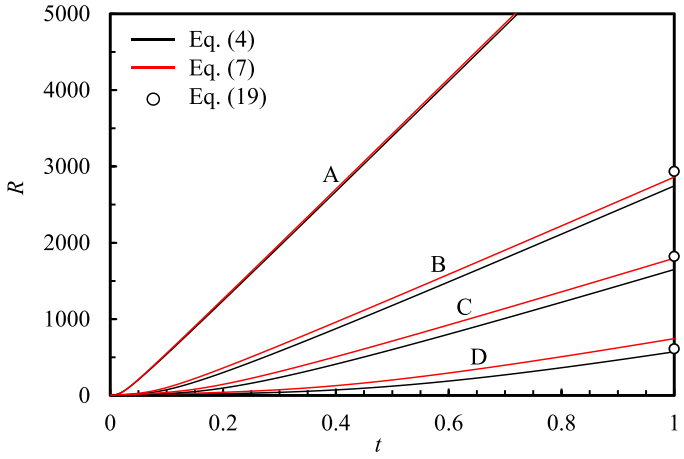

Figure 3. Comparison of equations (4) and (7) on temporal variations of the radius with $R_0 = 1$ $(1\ \mu\mathrm{m})$ under different tension strength in glycerol.

become small as the tension strength is increased, for example, the discrepancy is less than 0.6% for A (the strongest tension case), 4.2% for B, 9.0% for C, and 30% for D (the weakest tension case). Paying attention to acceleration times for A through D, we notice that they become longer as the tension strength is decreased, which reveals that the viscous term in (5) obtained by discarding the acceleration term in (4) was adopted in (6) in order to construct the model equation, in short, the longer the acceleration time, the larger the discrepancy. Therefore, the model equation has the limitation in accuracy depending on the viscosity and the tension strength; for reference, the viscosity-tension ratio is respectively $\mu/\Delta P = 5.996 \times 10^{-3}$ for A, 2.998×10^{-2} for B, 5.996×10^{-2} for C, and 1.578×10^{-1} for D. However, such limitation in weaker tension states is not fatal because the model equation is constructed by focussing solely on the dynamical cavitation threshold under very strong tension states as diesel fuel atomization or other similar phenomena.

Figure 3 compares (4) and (7) on the nucleus radii up to $t = 1$ for A, B, C, and D in figure 2. The black lines are obtained by solving (4), whilst the red lines are obtained by solving (7). The white circles represent the radii evaluated by analytical formula at $t = 1$, (19), which will be derived in the next section. For A, which is near the conditions dealt with by Gianndakis *et al* (2008), the radius attains 7.0×10^3 at $t = 1$ and (4), (7), and (19) coincide well with each other within 0.6%. In summary, the model equation can predict the growth behaviour of the nucleus when tension is strong.

3. Parametric classification of nucleus growth under strong tension

3.1. Detailed and global growth behaviour of nucleus for $(\Delta P + p_v)/\mu^2 \ll 1$

Before proceeding to analysis of the model equation (7), we should emphasize again that cavitation threshold under tension is the global growth process of a bubble nucleus up to $R \gg 1$ in the time domain $[0, 1]$, as shown in figures 2 and 3. However, we will inspect not only the global behaviour but also the detailed one just after the growth start as precisely as possible. We will here focus on the growth behaviour of the nucleus for the case A shown in figures 2 and 3: $\Delta P = 7.955 \times 10^7$ $(10\ \mathrm{MPa})$. Paying attention to the orders of $p_{g0}/\mu^2 = \mathrm{O}\left(10^{-3}\right)$,

$(\Delta P + p_v)/\mu^2 = \mathrm{O}\left(10^{-4}\right)$, and $\sigma/\mu^2 = \mathrm{O}\left(10^{-6}\right)$, we can approximate (7) is for $\mathrm{d}R/\mathrm{d}t > 0$ and $R = \mathrm{O}(1)$ as:

$$\frac{\mathrm{d}R}{\mathrm{d}t} \sim \frac{3p_{g0}}{\mu}\frac{\ln R}{R^2} + \frac{\Delta P + p_v}{\mu}R, \tag{8}$$

where the second term on the right-hand side of (8) is approximated as $1 - 1/R^3 \sim 1$. Thus, (8) may lack accuracy in the neighbourhood of $R = 1$. The first term of (8) is a gas-viscosity coupling term, and the second term is a tension-viscosity coupling term. As numerically estimated above, (8) holds under the conditions:

$$\frac{\Delta P + p_v}{\mu^2} \ll 1, \tag{9}$$

and $R = \mathrm{O}(1)$; giving a short comment to (9), its inverse case, i.e. $\mu^2/(\Delta P + p_v) \ll 1$, is the case for water, which is relevant to cavitation threshold in submerged water jets (Peng *et al* 2019) and purification of sewage water (Soyama 2021).

We now consider the extremes for (8), radii for which can be obtained from the transcendental equation, $(\Delta P + p_v)R^3/(3p_{g0}) - 2\ln R + 1 = 0$, resulting in $(\mathrm{d}R/\mathrm{d}t)_{\max} = 1208$ at $R = 1.824$ and $(\mathrm{d}R/\mathrm{d}t)_{\min} = 1095$ at $R = 3.612$, and the two terms on the right-hand side in (8) become balanced at $R = 1.038$ and $R = 3.297$. Inspecting details about which term prevails in the growth, we can understand that the growth is subject to the tension-viscosity coupling term between $R = 1$ and $R = 1.038$ and beyond $R = 3.297$, whilst it is subject to the gas-viscosity coupling term between $R = 1.038$ and $R = 3.297$. The tension-viscosity coupling term dominates $(93\,\%)$ at $R = 10$ up to which (8) approximately holds, as will be clarified below. Based on the above discussion, we can understand that the spike-like small protuberances near the origin seen in figure 2 are all the appearance of $(\mathrm{d}R/\mathrm{d}t)_{\max}$.

For $R \gg \mathrm{O}(1)$, on the other hand, if $(\Delta P + p_v)/\mu$ is large, (7) may be approximated as:

$$\frac{\mathrm{d}R}{\mathrm{d}t} \sim -\frac{\mu}{3R} + \left[\left(\frac{\mu}{3R}\right)^2 + \frac{2}{3}(\Delta P + p_v)\right]^{1/2}, \tag{10}$$

where the condition (9) is sufficiently fulfilled because of $(\Delta P + p_v)/\mu^2 \sim \mathrm{O}\left(10^{-4}\right)$ and both viscous (the terms with $\mu/3R$) and the tension (the term with $\Delta P + p_v$) effects control the velocity; the viscous effect decays as the nucleus grows and an inviscid behaviour is expected when $R \to \infty$.

Figure 4 plots $\mathrm{d}R/\mathrm{d}t$ against R for the range of $R = 1 \sim 50$, where the black line $(R = 1 \sim 13)$ is the result of solving (8) and the red line is obtained by solving (7), and the blue line $(R = 8 \sim 50)$ is obtained by solving (10). As seen, (8) is a good approximation to (7) up to $R \sim 10$ whilst (10) is also a good approximation to (7) beyond $R \sim 10$, showing that (8) and (10) asymptotically become closest at $R \sim 10$. Hereafter, we will use the symbol R_{tr} in a general form instead of $R \sim 10$. Thus, $R_{\mathrm{tr}}\,(= 10)$ denotes the transition radius through which the growth mechanism changes from the gas-viscosity coupling behaviour to the tension-viscosity coupling one. It depends on the conditions given but is roughly $\mathrm{O}(10)$ independent of conditions, for example, even for water under weak tension (of about 0.1 MPa). The deviation of (8) from (7) beyond R_{tr} is due to the breakdown of the assumption, $(\mu/3R)^2 \gg 2(\Delta P + p_v)/3 + 2p_{g0}\ln R/R^3$, whilst the deviation of (10) from (7) before R_{tr} is due to the neglect of $2p_{g0}\ln R/R^3$ in (10). Summarizing the results, we understand that (8) is rather exact for the gas-viscosity coupling growth up to R_{tr} whilst (10) is rather exact for the tension-viscosity coupling growth beyond R_{tr}. After R_{tr}, (10) soon approaches (7) and varies up to $t = 1$ $\left(R = 7.0 \times 10^3\right)$ along the curve A shown in figure 2, which means that (10) is valid for $R > R_{\mathrm{tr}}$.

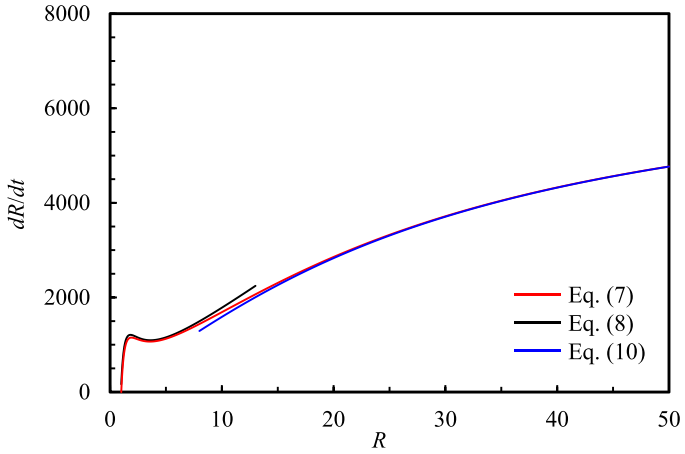

Figure 4. Comparison among (7), (8), and (10) for temporal variations of the growth velocity for the nucleus with $R_0 = 1$ (1 μm) under $\Delta P = 7.955 \times 10^7$ (10 MPa) in glycerol. The growth is subject to the gas-viscosity coupling term up to $R = 3.297$, after that the tension-viscosity coupling term prevails up to $R_{\rm tr}\,(= 10)$.

3.2. Classification of dynamical cavitation threshold

As clarified in the section 3.1, (10) prevails in the domain $[R_{\rm tr},\ R_1]$ in which R_1 is the radius at $t = 1$. Its solution in $[R_{\rm tr},\ R_1]$ is given as (note that $R_{\rm tr}$ is the known quantity as evaluated in 3.1, whilst R_1 is a quantity to be sought):

$$t\,(R_{\rm tr}) + F(R_1) = 1, \tag{11}$$

where:

$$t\,(R_{\rm tr}) = \frac{2\mu}{\frac{R_{\rm tr}+1}{R_{\rm tr}-1}\,(\Delta P + p_v) + \frac{6p_{g0}}{(R_{\rm tr}-1)^2}\left[1 - \frac{\ln R_{\rm tr}+1}{R_{\rm tr}}\right]}, \tag{12}$$

$$F(R_1) = \sqrt{\frac{3}{2\,(\Delta P + p_v)}}\left(\sqrt{R_1^2+\alpha} - \sqrt{R_{\rm tr}^2+\alpha}\right) + \frac{\mu}{2\,(\Delta P + p_v)}\ln\left[\left(\frac{R_1}{R_{\rm tr}}\right)^2 \frac{\sqrt{R_{\rm tr}^2+\alpha}+\sqrt{\alpha}}{\sqrt{R_1^2+\alpha}+\sqrt{\alpha}}\right], \tag{13}$$

in which:

$$\alpha = \frac{\mu^2}{6\,(\Delta P + p_v)}, \tag{14}$$

and $t\,(R_{\rm tr})$ is the time obtained from the radius variation $(R_{tr} - 1)$ and the mean growth velocity during the radius changing, the latter of which is derived from (8); $t\,(R_{\rm tr}) = 6.977 \times 10^{-3}\,(\ll 1)$ for the conditions given in 3.1, and $F\,(R_1)$ denotes the time while the nucleus grows from the radius $R_{\rm tr}$ to R_1. For the conditions, (11) can be approximated as:

$$\sqrt{\frac{3}{2\Delta P}}R_1 + \frac{\mu}{2\Delta P}\ln\left[\left(\frac{R_1}{R_{\rm tr}}\right)^2 \frac{\sqrt{{R_{\rm tr}}^2+\alpha}+\sqrt{\alpha}}{R_1}\right] \sim 1. \tag{15}$$

Let us rearrange the second term on the left-hand side of (15) by grouping the known and unknown terms as:

$$\sqrt{\frac{3}{2\Delta P}}R_1 + \frac{\mu}{2\Delta P}\ln\beta R_1 = \Pi, \tag{16}$$

where:

$$\Pi = 1 - \frac{\mu}{2\Delta P}\ln\frac{2}{3}\mu, \tag{17}$$

$$\beta = \frac{1}{R_{\rm tr}\sqrt{\Delta P}}\left(\sqrt{\frac{9\Delta P}{4\mu^2} + \frac{3}{8{R_{\rm tr}}^2}} + \sqrt{\frac{3}{8{R_{\rm tr}}^2}}\right). \tag{18}$$

Equation (16) is more compact than (15) because the second term of (15) is split into $(\mu/2\Delta P)\ln(\beta R_1)$ and $(\mu/2\Delta P)\ln(2\mu/3)$, in which $(\mu/2\Delta P)\ln(\beta R_1)$ is unknown whilst $(\mu/2\Delta P)\ln(2\mu/3)$ is known; the first term of (16), i.e. $\sqrt{3/2\Delta P}R_1$, is unknown. The parameter Π defined by (17) represents the measure for effects of the viscosity and the tension strength on the nucleus growth. Therefore, we may be able to find out a simpler threshold condition for $(\mu/2\Delta P)\ln(2\mu/3) \ll 1$, depending on magnitudes and signs of $(\mu/2\Delta P)\ln(\beta R_1)$. For example, for the case of figure 4, $(\mu/2\Delta P)\ln(2\mu/3) = 3.800\times10^{-2}$, thus, $\Pi \sim 1$ and $\beta = 7.056\times10^{-6}$, thus, $(\mu/2\Delta P)\ln(\beta R_1) = -9.018\times10^{-3}$, resulting in $R_1 \sim \sqrt{2\Delta P/3}$. This is the simplest case of (16). On the other hand, in case where $(\mu/2\Delta P)\ln(2\mu/3)$ is larger than 1, Π becomes negative, which is the case of tension weaker than D in figures 2 and 3. Summarizing the above discussion, we can classify (16) into the more perspective cases according to numerical value and signs of the parameters Π and $(\mu/2\Delta P)\ln(\beta R_1)$.

(1) In case where $\Pi > 0$ and Π is not too small compared with unity

This is the case where numerical value of Π is close to one, in other words, $\mu/\Delta P \ll 1$ and $(\mu/2\Delta P)\ln(\beta R_1) \sim {\rm O}\left(10^{-2}\right)$; for example, the case of figure 4. Then, we obtain R_1 from (16) as:

$$R_1 \sim \sqrt{\frac{2\Delta P}{3}}\Pi. \tag{19}$$

Equation (19) denotes that the nucleus radius attained during tension application is dominated by not only the tension strength but also the viscosity through the parameter Π. For the conditions given in figure 4, $\Pi = 0.962$ and $R_1 = 7.0\times10^3$ (7 mm in dimensional value). As the numerical value of Π is close to 1, the nucleus growth is almost governed by the tension, not the viscosity. Thus, we understand, from (10) and the present result, that the bubble during the tension duration continues to grow between $R \gg \mu/(3\sqrt{2\Delta P/3})$ and $R_1 = 7.0\times10^3$ as if it grows in an inviscid liquid; ${\rm d}R/{\rm d}t \sim \sqrt{2\Delta P/3} = $ constant. Then, the tension strength can be obtained from (17) and (19) as:

$$\Delta P \sim \frac{1}{2}\left[\frac{3}{2}R_1^2 + \mu\ln\frac{2}{3}\mu + \sqrt{\left(\frac{3}{2}R_1^2 + \mu\ln\frac{2}{3}\mu\right)^2 - \left(\mu\ln\frac{2}{3}\mu\right)^2}\right], \tag{20}$$

by which we can evaluate the tension strength needed for the nucleus growing up to the radius R_1 for the tension duration. This equation is useful for predicting the tension strength for the radius R_1 we want to have.

Figure 5 shows the relation of R_1 and ΔP, obtained by (20), between $R_1 = 5.0\times10^2$ (0.5 mm) and $R_1 = 1.0\times10^4$ (10 mm) for $R_0 = 1$ (1 μm). From this figure, we can predict the tension strength under which the nucleus grows up to a certain radius. In the figure,

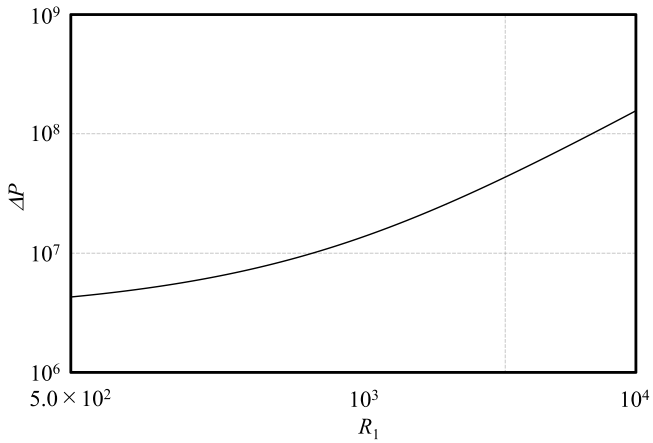

Figure 5. Relation between R_1 and ΔP between $R_1 = 5.0 \times 10^2$ (0.5 mm) and $R_1 = 1.0 \times 10^4$ (10 mm) for $R_0 = 1$ (1 μm) in glycerol.

the initial nucleus radius is given to be the above value, but it will be demonstrated in subsection 3.5 that the initial radius does not influence the radius R_1 when tension is strong.

(2) In case of $\Pi = 0$

Equation (16) is then reduced to:

$$\sqrt{\frac{3}{2\Delta P}} R_1 + \frac{\mu}{2\Delta P} \ln \beta R_1 = 0, \tag{21}$$

which is the transcendental equation and the case of $\Delta P = 3.022 \times 10^6$ (0.380 MPa), for which $R_1 \sim 6.1 \times 10^2$ (0.61 mm). The tension and viscosity effects both prevail in the nucleus growth. For a further development of tension-viscosity coupling growth, we need to prolong the reference time. As discussed, about curve D in figures 2 and 3, this case is not accurate because the growth is still accelerating, due to weak tension, where the model equation is barely valid. Yet, the result might be informative.

(3) In case of $\Pi < 0$

This is the case $\Delta P < 3.022 \times 10^6$ (0.380 MPa) and the model equation becomes inaccurate for the smaller tension strength. Thus, considering the inaccuracy of (7) and the insufficient nucleus growth under the weak tension $(\Delta P < 3.022 \times 10^6)$, the case of $\Pi < 0$ may not be so meaningful in cavitation threshold.

In summary, the most important result in this subsection is the case (1) where the tension prevails for cavitation threshold and the model equation holds. For the case (2), the equation is barely valid because the nucleus growth is still in the acceleration process, nevertheless, it is useful. Note that the conditions discussed here for glycerol are not the case for water at high temperatures and weak tension; then we must return to (11) through (14).

3.3. Dynamical cavitation threshold and Blake's quasistatic threshold

As discussed in Introduction, Blake's threshold is known well (Young 1999, Franc and Michel 2005, Brennen 2013), which is constructed for the situation that a nucleus grows from the

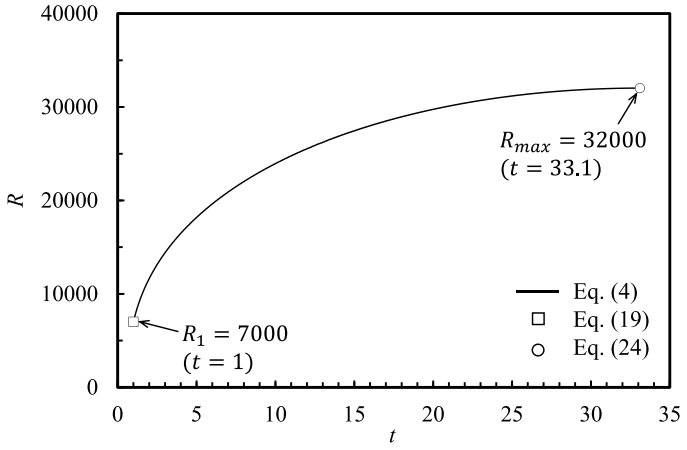

Figure 6. Behaviour of the nucleus with $R_0 = 1$ (1 μm) in glycerol while the liquid pressure restores to the atmospheric pressure (7.955×10^5 (0.1 MPa)).

instant when the liquid pressure is reduced to a certain value for an infinite time in a quasistatic manner:

$$R_c = \sqrt{\frac{3p_{g0}}{\sigma}}, \tag{22}$$

$$p_c = p_v - \frac{2\sigma}{3R_c}, \tag{23}$$

where R_c is called the critical radius and p_c is the critical pressure; both are nondimensionalised. These equations imply that the nucleus continues to grow after its radius attains R_c when the liquid pressure is kept at p_c above which the radius varies in equilibrium with the ambient pressure. For the initial nucleus radius and initial liquid pressure given in figure through 4, $R_c = 4.866 \times 10$ (4.866×10 μm) and $p_c = -1.382 \times 10^4$ $\left(-1.737 \times 10^3\,\text{Pa}\right)$. Comparing the tension strength for this case ($\Delta P = -p_c > 0$) with the tension values for the case (1) and the case (2) in the preceding section 3.2, we understand that the tension strength evaluated by Blake's threshold is far less than the values evaluated by our dynamical threshold, which means that a tension stronger than that of Blake's threshold is required in cases of finite durations of tension, that is, the dynamical threshold; however, note that Blake's threshold is the important condition necessary for the nucleus starting to grow.

3.4. Bubble behaviour under atmospheric pressure after the tension release

We can evaluate the maximum bubble radius $R_{\max}$ when the liquid pressure again restores in the stepwise fashion to a high pressure p_a (here, for brevity an atmospheric pressure) after the tension was released (Fujikawa *et al* 2019):

$$R_{\max} \sim R_1 \left(\frac{\Delta P}{p_a}\right)^{1/3}, \tag{24}$$

where $R_1 = 7.0 \times 10^3$ and $\Delta P = 7.955 \times 10^7$ for the case of figure 4 and $p_a = 8.059 \times 10^5$, resulting in $R_{\max} \sim 3.2 \times 10^4$ (32 mm). The predicted maximum radius shown by the white circle is compared with the numerical solution of (4), the solid line, in figure 6. The bubble

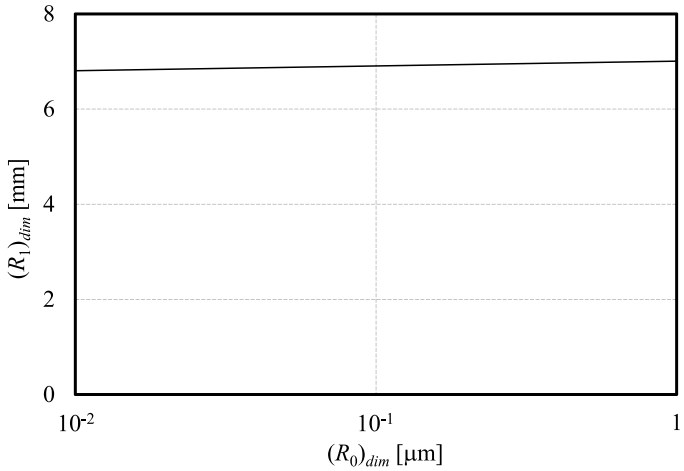

Figure 7. Relation between $(R_0)_{\rm dim}$ and $(R_1)_{\rm dim}$ for $(R_0)_{\rm dim} = 10^{-2}\ \mu$m $\sim 1\ \mu$m and $(\Delta P)_{\rm dim} = 10$ MPa $\left(7.955 \times 10^7\right)$ in glycerol.

nucleus attains the maximum radius at $t = 33.1\ (3310\ \mu s)$. For reference, the radius evaluated by (19) at $t = 1\ (100\ \mu s)$ is presented by the white square. Relative errors between the two predicted values and the numerical solution of (4) are less than $1.17\,\%$. The nucleus continues to grow even under the atmospheric pressure up to the large size for the longer period after the tension was released. At the maximum radius, the pressure of the gas is 2.4×10^{-5} which is far lower than the vapor pressure $\left(p_v = 9.228 \times 10^{-2}\right)$, producing strong shock waves repeatedly during shrinking phases where the R-P equation becomes invalid as the liquid compressibility prevails (Fujikawa and Akamatsu 1980). Note that the nucleus is supposed to grow in an infinite space of liquid. Its behaviour in a confined space of liquid is discussed in the thesis by the second author (Fujikawa 1980).

3.5. Effects of tension strength and duration, viscosity, density, and nucleus radius on dynamical cavitation threshold

Again, let us return to (19) for the case where $\Pi > 0$ and Π is not too small compared with unity. Hence, in terms of dimensional quantities it reads:

$$(R_1)_{\rm dim} \sim \left[T\sqrt{\frac{2\Delta P}{3\rho}} \left(1 - \frac{2\mu}{T\Delta P} \ln \frac{8}{3} \frac{\mu T}{\rho R_0^2} \right) \right]_{\rm dim}, \tag{25}$$

where the subscript dim denotes the dimensional quantities. Equation (25) indicates that the bubble radius attained during the tension application is expressed by the tension strength and duration, the viscosity, the density, and the nucleus radius. The nucleus grows to the maximum radius proportionally to both the tension duration and the square root of the tension strength, and the growth is hardly influenced by the initial nucleus radius because the second factor in the round brackets changes in the logarithmic-varying manner of $(R_0)_{\rm dim}$ together with the viscosity, the density, and the tension duration; $\ln(8\mu T/3\rho R_0^2) \sim {\rm O}(10)$ for $(R_0)_{\rm dim} = 10^{-2}\mu$m $\sim 1\mu$m and $2\mu/T\Delta P \sim 3 \times 10^{-3}$.

Figure 7 shows the relation between $(R_0)_{\rm dim}$ and $(R_1)_{\rm dim}$ for $(R_0)_{\rm dim} = 10^{-2}\ \mu$m $\sim 1\ \mu$m and $(\Delta P)_{\rm dim} = 10$ MPa $\left(7.955 \times 10^7\right)$ and clearly demonstrates that $(R_1)_{\rm dim}$ and $(R_0)_{\rm dim}$ are

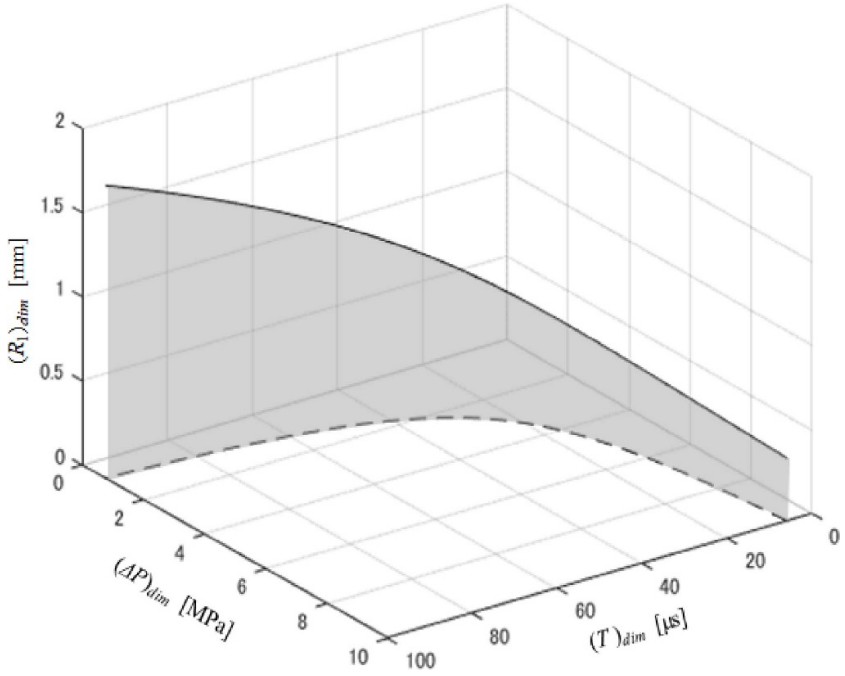

Figure 8. Three dimensional features among $(\Delta P)_{\rm dim}$, $(T)_{\rm dim}$, and $(R_1)_{\rm dim}$ for $\Pi = 0.5$ and $(R_0)_{\rm dim} = 1\,\mu$m in glycerol.

hardly correlated. Such indifference of nucleus radius to the grown bubble radius was pointed out by Gianndakis *et al* (2008) although the reason has remained unclear. However, from figure 7, we understand that the dynamics of the nucleus grown up to the large radius $(R_1)_{\rm dim}$ is fully controlled by the tension and the nucleus grows at a constant speed (see the curve A in figure 2), in consequence, its growth in this stage is free from the initial radius of the nucleus.

Figure 8 shows three dimensional features among $(\Delta P)_{\rm dim}$, $(T)_{\rm dim}$, and $(R_1)_{\rm dim}$ in case where $\Pi = 0.5$ and $(R_0)_{\rm dim} = 1\,\mu$m. The figure is depicted on the $(\Delta P)_{\rm dim} - (T)_{\rm dim}$ plane by the relation:

$$(\Delta P)_{\rm dim} \sim \left(\frac{4\mu}{T} \ln \frac{8}{3} \frac{\mu T}{\rho R_0^2} \right)_{\rm dim}, \tag{26}$$

and the relation $(R_1)_{\rm dim} \sim 0.5 \left(T\sqrt{2\Delta P/\rho} \right)_{\rm dim}$ against the $(\Delta P)_{\rm dim} - (T)_{\rm dim}$ plane. Equation (26) is obtained from (25) for $\Pi = 0.5$ and holds for $(R_0)_{\rm dim} = 10^{-2}\ \mu$m $\sim 1\ \mu$m, as shown in figure 7. Figure 8 clearly demonstrates that the larger the tension strength, the shorter the tension duration for the parameter fulfilling $\Pi = 0.5$, and the smaller the bubble radius attained during the tension application. The grown bubble is visible. Like this example, we can predict the bubble radius for a supposed tension strength and a duration, which enable us to evaluate the radius of the grown-up bubble under the supposed tension strength and the duration for configurations of experimental facilities; figures like figure 8 can be depicted for any values of Π and are informative for the design of the facilities.

Finally, the tension strength and its duration depend on both given conditions and configurations for fuel injector nozzles in diesel engines. Therefore, we should first understand a nozzle performance by, for example, CFD simulations as correctly as possible and evaluate

the growth behaviour of bubble nuclei in the nozzles. Only thereafter, we may find optimal conditions applying the dynamical cavitation threshold theory proposed in this paper.

4. Conclusions

We presented details of dynamical cavitation threshold for vapor-gas bubbles in glycerol under a finite duration of strong tension based on the bubble- dynamical model equation. The equation was examined for different tension values. It was observed that discrepancies between the R-P equation and the model equation diminish as tension imposed on glycerol becomes stronger. The model equation is found to be valid in cases of strong tension with which the threshold is concerned. We classified the threshold into three patterns according to signs and numerical value of the parameter defined by the viscosity and the tension strength. The maximum radii attained during the tension application were given in simple formulae for the cases where the threshold was concerned with. The results suggested that the nucleus radius attained is completely dominated by the parameter and cavitation threshold for usual conditions takes place in later stages of the tension and viscosity-controlled growth. We also elucidated that the tension strength needed for the nucleus growing to a certain size is expressed by both the viscosity and the bubble radius we want to obtain, which is the useful result for performance optimization of fuel injector nozzles. The discrepancy between the dynamical threshold and Blake's threshold was elucidated. The dynamical threshold theory was applied to cavitation situations and how to use it was demonstrated through the examples. The theory will be useful for not only the diesel fuel atomization but also understanding cavitation threshold experiments based on Washio's method (Washio 2014) and applications to submerged water jets (Peng *et al* 2019) and purification of sewage water (Soyama 2021). Furthermore, as discussed in the subsection 3.5, cavitation threshold is strongly dependent on tension durations, suggesting that, in actual flow situations, the threshold of bubble nuclei may be affected by places where the nuclei exist in the flow under tension—in the main flow or inside the boundary layer. This is a challenging issue of the threshold in the near future.

Finally, we successfully applied our model equation to the dynamical cavitation threhold for glycerol in this paper, but we recommend that the equation should be validated by compring it with the R-P equation for unexamined liquids where we will be in uncharted waters; the model equation has been ascertained to be valid for water, liquid hydrogen, liquid oxigen, olive oil, and glycerol for strong tension until the present.

Acknowledgments

This work was financially supported in part by the grant of JSPS KAKENHI (Grant No. 20K04296) in 2021 and that from Toyohashi University of Technology in 2021. The first author would like to cordially appreciate these grants.

References

Brennen K 2013 *Cavitation and Bubble Dynamics* (Oxford: Oxford University Press) (https://doi.org/10.1017/CBO9781107338760)

Franc J-P and Michel J-M 2005 *Fundamentals of Cavitation* (Kluwer Academic Publishers) (https://doi.org/10.1007/1-4020-2233-6)

Fujikawa S 1980 Studies on the mechanisms of cavitation bubble collapse *PhD Thesis* Kyoto University

Fujikawa S and Akamatsu T 1980 Effects of non-equilibrium condensation of vapour on the pressure wave produced by the collapse of a bubble in a liquid *J. Fluid Mech.* **97** 481–512
Fujikawa T, Egashira R, Yaguchi H and Fujikawa S 2019 Parametric classification and prediction method of cavitation inception under a tension for a finite time and subsequent atmospheric pressure (in Japanese) *Turbomachinery* **47** 52–60
Gianndakis E, Gavaises M and Arcoumanis C 2008 Modelling of cavitation in diesel injector nozzles *J. Fluid Mech.* **616** 153–93
Mørch K A 2015 Cavitation inception from bubble nuclei *Interface Focus* vol 5 (The Royal Society Publishing) pp 1–13
Peng G, Mori M, Tazaki T and Oguma Y 2019 Numerical simulation of unsteady cloud cavitation: a comparative study of compressible mixture models *Earth Environ. Sci.* **240** 62043
Soyama H 2021 Luminescence intensity of vortex cavitation in a Venturi tube changing with cavitation number *Ultrason Sonochem.* **71** 105389
Sun Y, Guan Z and Hooman K 2021 Cavitation in diesel fuel injector nozzles and its influence on the atomization and spray *Chem. Eng. Technol.* **42** 6–29
Washio S 2014 *Recent Developments in Cavitation Mechanisms—A Guide for Scientists and Engineers* (Woodhead Publishing) (https://doi.org/10.1016/C2013-0-18235-9)
Yasui K 2018 *Acoustic Cavitation and Bubble Dynamics* (Berlin: Springer-Nature) (https://doi.org/10.1007/978-3-319-68237-2)
Young F R 1999 *Cavitation* (Imperial College Press) (https://doi.org/10.1142/p172)